Polym. Bull. (2009) 62:713–725
DOI 10.1007/s00289-009-0049-8

ORIGINAL PAPER

Preparation and characterization of blend membranes of polyurethane and superfine chitosan powder

Dan-Ying Zuo · Yong-Zhen Tao · Yu-Bo Chen · Wei-Lin Xu

Received: 7 September 2008 / Revised: 6 January 2009 / Accepted: 8 February 2009 /
Published online: 15 February 2009

Abstract A novel kind of asymmetric blend membranes with superfine chitosan powder (SCP) and biomedical polyurethane was prepared by immersion precipitation phase inversion method. Effects of different SCP content on the morphology and properties of the blend membranes were investigated. The result showed that SCP content had little influence on the cross-section structure of the blend membranes, and the cross-section presented a cellular structure. WAXD results revealed that the aggregated structure of SCP remained. With an increment of SCP content, the pore diameter and porosities of blend membranes increased firstly, and then decreased. While, the water absorption rate and water vapor transmission rate were improved remarkably with increasing SCP content. The mechanical testing results indicated that with an increment of SCP ratio, mechanical properties presented a descending trend, whereas all blend membranes exhibited the good elasticity.

Keywords Chitosan superfine powder (SCP) · Polyurethane (PU) · Blend membrane · Phase inversion

Introduction

Chitosan, the alkaline *N*-deacetylated derivative of chitin, is one of the most abundant naturally polysaccharides, and it has been proved to be biologically renewable, biodegradable, biocompatible, non-antigenic, non-toxic, and bio-

D.-Y. Zuo · Y.-Z. Tao · Y.-B. Chen · W.-L. Xu (✉)
Key Laboratory for Green Processing and Functional Textile of New Textile Materials,
Ministry of Education, Wuhan University of Science and Engineering,
430073 Hubei, People's Republic of China
e-mail: wusems419@yahoo.com.cn

functional. At present, chitosan has been widely studied for biomedical applications [1–3]. However, the rapid degradation and the low hygrometric mechanical property of chitosan limit its use [4, 5]. To overcome this limitation, chitosan generally has been blended with other polymer. It has been shown that the blending chitosan-based materials exhibited combinations of properties that could not be obtained by individual polymers and the mechanical properties as well as the biological effects on cells will be varied in the blended materials [6, 7]. Since molecular chains of chitosan are rigid and decomposition temperature is lower than the melting temperature, melting blending was unsuitable for chitosan. Chitosan could solve in a few kinds of dilute acidic aqueous solutions, so solution blending was used for chitosan blending with other polymer. Blending polymers could be water-soluble and natural or synthetic including collagen, glucomannan, polyvinyl alcohol, polyethylene oxide, poly(vinyl pyrrolidone) and so on. These researches results revealed that the intermolecular interaction (hydrogen bonding or ionic bonding) between chitosan and other polymers occurred. But there was a phase separation in the blending materials. So, in order to obtain good miscibility, the blending polymer content is very low [8–11].

On the other hand, biomedical polyurethane (PU) offers the specific properties such as physiological acceptability, excellent blood compatibility, excellent stability over long implant periods and excellent physical and mechanical properties, etc. Therefore, PU has frequently been used as a promising biomaterial such as vascular grafts, catheters, general-purpose tubing and artificial hearts et al. [12, 13]. The blend of chitosan and PU could provide more outstanding physiological and mechanical properties. But, biomedical PU only solve in some organic solvents and chitosan solution is a non-solvent for PU solution, so chitosan solution cannot be fairly well dispersed in PU matrix, but induced PU solution precipitation as coagulant.

In this study, in order to obtain the membrane with high chitosan content, the porous blend membranes were fabricated by using superfine chitosan powder (SCP) blending with PU solution, not chitosan solution and PU solution, through the immersion precipitation phase inversion method. Superfine powder is defined as all of the powder smaller than 30 μm in diameter [14]. With the further understanding of the special properties of superfine powder and the development of processing technologies, there have been many extensive applications of superfine powder including organic and inorganic materials in modern industries and related hi-tech fields [15–17]. For example, silk fibroin superfine powder has already found its utility as cosmetic materials and functional foods because of its moderate moisture absorption and retention properties, and its high affinity for human skin and silk [18]. Actually, chitosan powders also preserve these virtues. PU/chitosan blend membrane was prepared by using a kind of self-made organic SCP in this study. This research discussed the effects of the mass ratio of SCP to PU on the structure and properties of SCP/PU membranes. The microstructure, the swelling capacity, the water vapor transmission rate (WVTR), as well as the tensile properties of SCP/PU membrane were investigated.

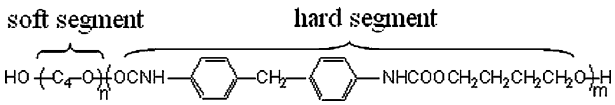

Fig. 1 Structure of medical PU (Pellethane® 2363-80AE)

Experimental

Materials

Chitosan with degree of deacetylation 90% (M_η = 54 kD) made from shrimp was purchased from Bangcheng Chemical Co. Ltd, Shanghai, China, PU of medical grade (Pellethane 2363-80AE) was supplied by Dow Chemical Corporation, and its structure was shown in Fig. 1. *N*, *N*-dimethyl formamide (DMF) of analytical grade was obtained from Guoyao Chemical Co. Ltd, Shanghai, China. Distilled and deionized water was used throughout this study.

Preparation and characterization of superfine chitosan powder (SCP)

Chitosan was milled into chitosan superfine powder (SCP) by a self-made millstone [19]. Laser analyzer (Powder Analyse Instrument JL-1166, China) was used to measure the average particle size and size distribution of the SCP.

Preparation of SCP/PU blend membranes

SCP/PU blend membranes were fabricated using the method of immersion precipitation phase inversion at 25 °C. A certain amount of PU and DMF were stirred together in a rockered flask. After PU fully dissolved in DMF, SCP with various mass ratio to PU (0/100, 10/90, 30/70, 50/50, 70/30) was taken into the solution and stirred together until a homogeneous mixture was obtained. The flask was vacuumed to remove bubbles in the mixture, and then the mixture was cast into a 300 μm thick thin film on a clean glass plate, and the solution film was submerged in a gelation bath of distilled water overnight for allowing the exchange of solvent and non-solvent. After desiccation in air, membranes were removed from the glass plate. The blend membranes with the weight ratio of SCP to PU being 0/100, 10/90, 30/70, 50/50 and 70/30 were called a, b, c, d, and e.

Scanning electron microscopy

The dried membranes were fractured in liquid nitrogen. The morphologies in cross-section and the surfaces of the membranes were examined on a scanning electronic microscope (JSW-5610LV, Japan) after coating with gold under vacuum.

X-ray diffraction analysis

The crystallization in blend membranes was determined by wide-angle X-ray diffraction (WAXD) instrument (UltraIII, Rigaku, Japan) at the scanning rate of 4°/min. And the lamellar thickness (L) was calculated using the Scherrer equation

$$L = \frac{k\lambda}{B\cos\theta} \tag{1}$$

in which the structure factor $k = 1.0$, $\lambda = 0.154$ nm and B is the width at half maximum intensity of the crystal plane reflection [20].

Determination of membrane porosity

An overall porosity can be estimated with the area (A), the mass (W_m), the thickness (D) of membrane, and the density (ρ_p) of the polymer in membrane [21]. The mass and the thickness were measured with an electronic balance and a thickness gauge. The percentage porosity was calculated as follows:

$$\rho_P = \rho_1 \times a\% + \rho_2 \times b\% \tag{2}$$

$$\text{Porosity}\,(\%) = \frac{DA - (W_m/\rho_p)}{DA} \times 100\% \tag{3}$$

ρ_1 is density of PU, 1.12 g/cm^3. $a\%$ is PU percentage in blending polymer. ρ_2 is density of chitosan, 0.94 g/cm^3. $b\%$ is chitosan percentage in blending polymer. According to Eq. 1, ρ_p of polymer in five membranes is 1.12, 1.10, 1.06, 1.02, 0.99 g/cm^3, respectively. Porosity is expressed as the mean ± standard deviation ($n \geq 4$).

Water absorption tests

The water sorption capacities of SCP/PU blend membranes were determined by swelling the membranes in pH 7.4 of PBS at room temperature. A known weight of dry membrane sample (m_1) was immersed in the media for a certain time and was taken out. The wet sample was weighed (m_2) after the water on the sample surface was drained by filter paper. The percentage water absorption of samples in the media was then calculated from the formula Eq. 4.

$$Q = (m_2 - m_1)/m_1 \times 100\% \tag{4}$$

Water vapor transmission rate (WVTR)

The WVTR was measured according to the method used by Huang [22]. WVTR is calculated as following

$$\text{WVTR} = \frac{QC}{A} \times \frac{10^{-6}}{60} \times 1,000 \times 3,600 \times 24 \tag{5}$$

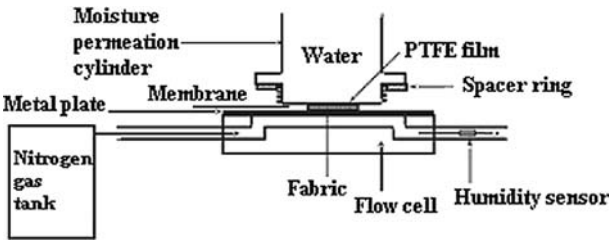

Fig. 2 Internal view of moisture permeation cylinder

where WVTR is the water vapor transmission rate of the sample (g/m^2 day), A is the area of the test sample (m^2), Q is the actual volumetric flow rate (cm^3/min), and C is the water vapor concentration of outgoing stream (kg/m^3). Internal view of moisture permeation cylinder was presented in Fig. 2.

Mechanical test

Mechanical tests of the blend membranes were performed on a tensile strength instrument (Instron5566, USA) at a crosshead speed of 50 mm/min. The width of the samples was 10 mm. The values are expressed as the mean ± standard deviation ($n \geq 4$).

Results and discussion

Characterization of superfine chitosan powder (SCP)

Figure 3 shows the particle size distribution of the SCP. It was apparent that the particle size of SCP was between 0.20 and12 μm, and the 72.5% of the powder is less than 4 μm, while the proportion of SCP with 1 and 2 μm particle sizes keeps 14.5 and 12.5%, respectively. The average particle size of SCP was calculated to 3.28 μm.

Porosity of SCP/PU blend membrane

The concentrations of all casting solutions were 20 wt%, and the mass ratio of SCP to PU varied from 0/100, 10/90, 30/70, 50/50 to 70/30. The viscosities of casting solutions, the porosities and thickness of different blend membranes are presented in Table 1.

Form Table 1, it is found that the porosities and thickness of membranes firstly increase and subsequently decrease with SCP mass ratio increasing. Chitosan with a large numbers of –OH and NH_2 groups is more hydrophilic. Therefore, with SCP content increasing and PU content reducing, more nonsolvent water was

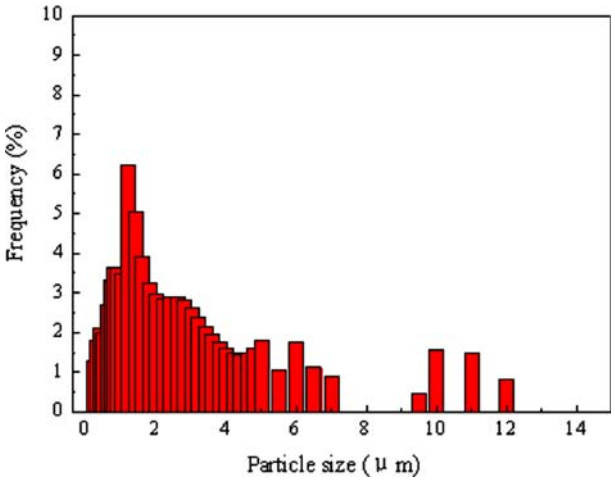

Fig. 3 Particle diameter distributing figure of SCP

Table 1 Properties of PU membrane and different SCP/PU blend membranes

Membrane sample	SCP/PU (wt/wt)	Viscosity of casting solution (Pa s)	Porosity (%)	Thickness (μm)
a	0/100	24.1	29.2 ± 0.4	100
b	10/90	7.9	48.2 ± 0.3	110
c	30/70	5.9	51.3 ± 0.5	130
d	50/50	1.6	50.1 ± 0.5	120
e	70/30	0.9	35.3 ± 0.5	115

absorbed to diffuse into solution films, and the nuclei of the formed poor-polymer phase progressed onwards rapidly and the precipitation rate of membrane-forming was improved, which was propitious to the porous membrane formation. On the other hand, with SCP ratio increasing, the viscosities of blend casting solutions decrease gradually as showed in Table 1. The viscosity decrease could elevate the exchange rate of solvent and non-solvent and the precipitation rate of the casting solution was enhanced, then the looser membrane formed easily with high porosity [23]. Consequently, duo to SCP mass ratio increasing, both the SCP hydrophilicity and the viscosity decrease of blended solutions made the precipitation rates of membrane-forming systems are quicker; so the SCP/PU blend membrane became more porous with porosities and thickness increasing. However, when SCP ratio exceeded 30 wt%, the congregation of mutual SCP was amplified, which could destroy the membrane pores. What's more, during the process of membrane drying, SCP specific surface area was enlarged; therefore, the disparity of shrinkage ratio of PU continuous phase with elastic deformation and SCP disperse phase with plastic behavior also was augmented because of SCP content increasing. Accordingly, a majority of the formed pores was broken and

collapsed, which resulted in SCP/PU blended membrane porosity and thickness reducing.

Morphology of SCP/PU blend membrane

Figure 4 reveals the SEM photos of membranes with different SCP/PU mass ratio. The upper surfaces of all SCP/PU membranes were dense, whereas, with SCP/PU ratio increasing, the upper surfaces of SCP/PU membranes became coarser. The SCP/PU ratio had an apparent influence on the bottom surfaces of blend membranes. When SCP content in polymer varied from 0 to 30 wt%, the pore diameter of the bottom surfaces increased gradually, and pore distribution was more uniform. The pore size distributed in a range of 5–7.5 μm for a membrane with SCP/PU ratio of 10–90, while, the pore size distributed in a range of 7.5–12.5 μm for b membrane with 30/70 of SCP/PU mass ratio. When SCP content increased to 50 wt%, the bottom surface of blend membrane became impact. The cross-sections of all blend membranes exhibited a cellular structure. However, as SCP content increasing to 50 wt%, the pore structure of cross-section became obscure and most of pores collapsed as shown in Fig. 4d3.

For SCP/PU mass ratio effects on the blend membrane structures, the result from SEM was same to that of porosity. With SCP/PU ratio increasing, pore size and porosity firstly increased and then reduced. The reason causing this phenomenon was that the different SCP/PU ratio had an effect on the phase transformation of the membrane-forming systems, as analysis in above. When SCP content changed from 0 to 30 wt%, the SCP hydrophlicity and the lowing viscosity quickened the precipitation rates, and the porous membranes were formed with higher porosities. However, when SCP content further increased to 50 and 70 wt%, the SCP stronger aggregating and SCP plastic deformation in the membranes during drying process brought about the pore collapse, accordingly, the denser membranes were fabricated with low porosities and small pore sizes.

Aggregated structure of SCP/PU blend membrane

Figure 5 presents diffraction curves of PU raw material, SCP raw material and SCP/PU blend membranes. The diffraction peaks of SCP appeared at 10.13°and 19.86°. And there was a diffraction wide peak at 20.88° for PU, which suggested that the crystallization degree of PU was very low. Independent of the ratio of SCP to PU, the diffraction peaks appeared at about 10°and 20° for all membranes. Meanwhile, the intensity of these two peaks increased with SCP ratio increasing. Compared with diffraction curves of SCP and PU raw materials, it can be deduced that two diffraction peaks of SCP/PU blend membranes were caused mainly by crystalline structure of the SCP. With SCP content increasing, the second peak shifted from 19.86° near PU diffraction peak to 20.10° near SCP diffraction peak. These results implied and the SCP aggregated structure was not destroyed during the processing.

Table 2 showed the crystalllinity and the lamellar thickness (L) of crystal panel at about 20° for SCP/PU blend membranes, PU and SCP raw material. With mass ratio increasing of SCP with the high crystallinity, the crystallinity of blend membranes

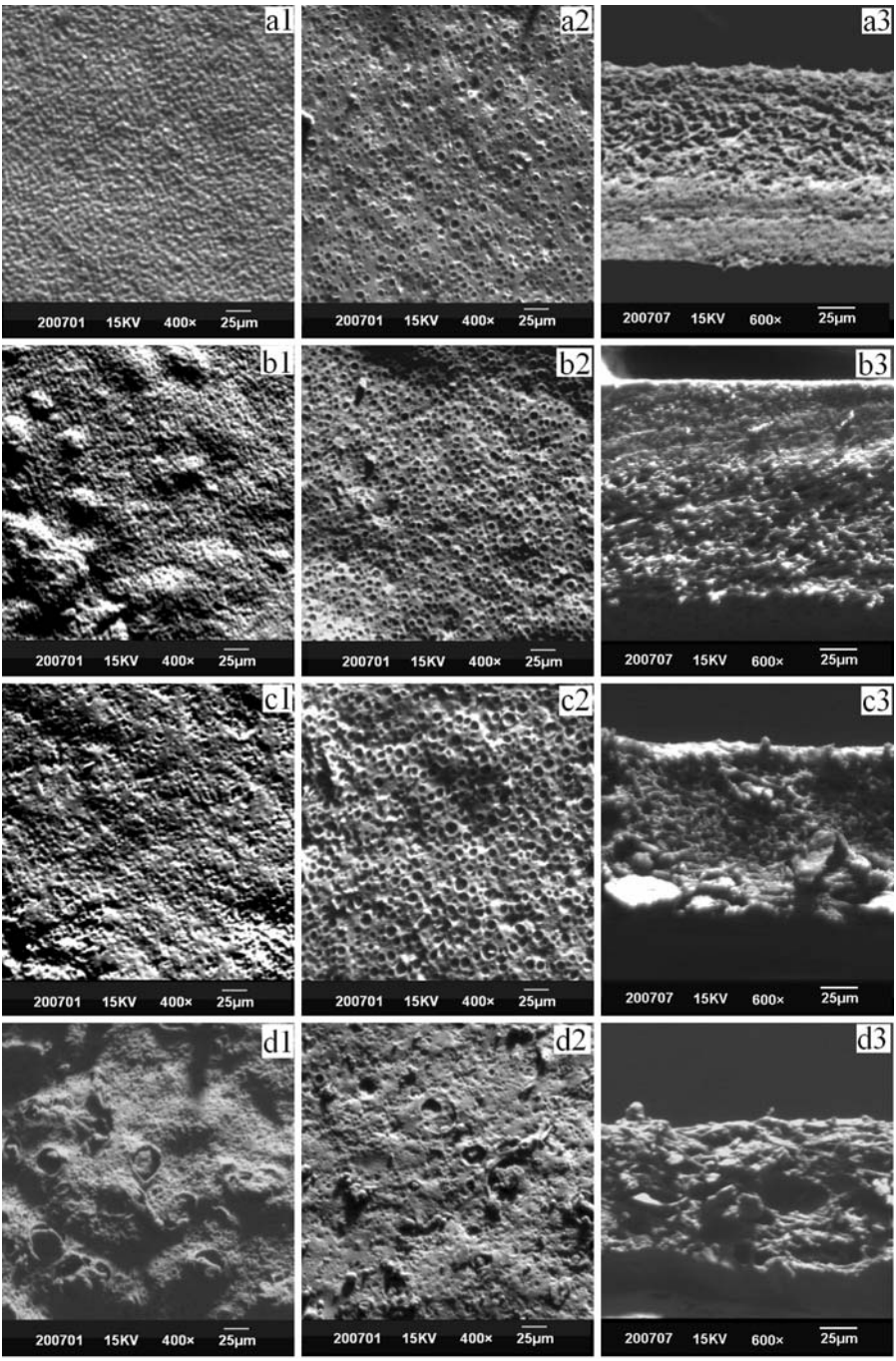

Fig. 4 SEM images of different SCP/PU blend membranes. **a** SCP/PU = 0/100, **b** SCP/PU = 10/90, **c** SCP/PU = 30/70, **d** SCP/PU = 50/50. *1* top surface, *2* bottom surface, *3* cross-section

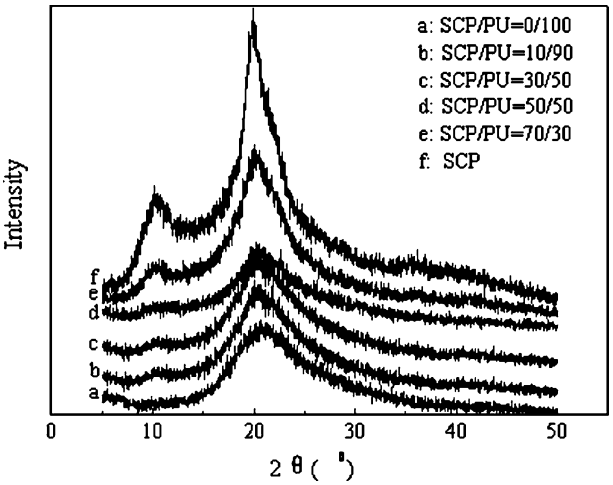

Fig. 5 WAXD spectrums of SCP/PU blend membrane, PU and SCP raw material

was elevated from 12.20 to 33.72%. On the other hand, *L* of crystals increased with SCP content augmenting. Since chitosan aggregated structure was remained, the change of the crystallite size resulted from the microstructure alteration of PU. The enlargement of L suggests that the SCP was trapped in the PU crystallite domain through hydrogen bonds between –OH and $–NH_2$ groups of SCP and –C=O and –NH– groups in PU chains.

Water absorption of blend membranes

The variations of water absorption of different SCP/PU membranes with time prolonging are shown in Fig. 6. Firstly, after immersed in media for initial 0.5 h, the swelling rates of membranes were very rapid with a nearly 90° slope of the curves of the absorption percentage–time. When samples were immersed for about 10 h, the water absorption of blend membranes reached a saturation platform, i.e., the equilibrium water absorption percentage. Secondly, with SCP/PU mass ratio increasing, the equilibrium water absorption percentage became higher. The

Table 2 Crystallinity and the lamellar thickness of SCP/PU blend membrane, PU and SCP raw material

Membrane sample	SCP/PU (wt/wt)	Crystallinity (%)	Lamellar thickness (*L*) (nm)
a	0/100	5.25	2.13
b	10/90	12.20	2.17
c	30/70	24.16	2.23
d	50/50	25.88	2.49
e	70/30	33.72	2.86
f	SCP	66.72	2.49

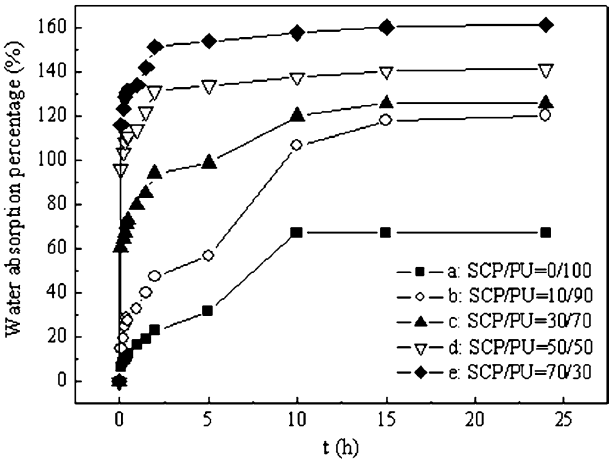

Fig. 6 Water absorption characteristics of different SCP/PU blend membranes

equilibrium water absorption percentage of pure PU membrane (a) was only 67.40%, however, for membranes with 10/90, 30/70, 50/50, 70/30 of SCP/PU mass ratio, and the equilibrium water absorption percentage increased to 120.52, 125.92, 141.51 and 161.50%, respectively. Chitosan chains contain abundant hydrophilic –OH and $–NH_2$ groups which easily absorb water molecules, therefore, with SCP ratio increasing in membranes, membranes could absorb more water and reached a higher equilibrium water absorption percentage. The other factor affecting water absorption was membrane structure. Here, with SCP/PU ratio changing, the porosity variation of membranes was inconsistent with that of membrane water absorption. As SCP content increasing 0–30 wt%, both porosities and water absorption percentage increased. But when SCP content further increased to 50 and 70 wt%, porosities of blend membranes decreased, whereas water absorption of blend membranes still enhanced. This suggested that SCP content was a major factor influencing the water absorption of blend membranes and the decrease of porosity had a negligible effect on it.

Water vapor transmission rate (WVTR) of blend membranes

With SCP content in polymer varying from 0 to 70 wt% in the blend casting solution, WVTR of blend membranes take on an ascending trend as shown in Fig. 7. WVTR of five membranes a–e were 1,933, 2,109, 2,566, 7,970 and 8,519 m^2 day, respectively. The permeation of water vapor through asymmetric membranes consists of two steps: adsorption and diffusion [24]. In general, adsorption concerns the membrane material hydrophilicity and chain structure of polymer, whereas diffusion relates to the pore morphology of membrane. With SCP content increasing to 30 wt%, WVTR of blend membranes increased, which attributed to the improvement of the porosities and hydrophilicity of blend membranes. The improvement of the porosity and hydrophilicity can accelerate the rates of water

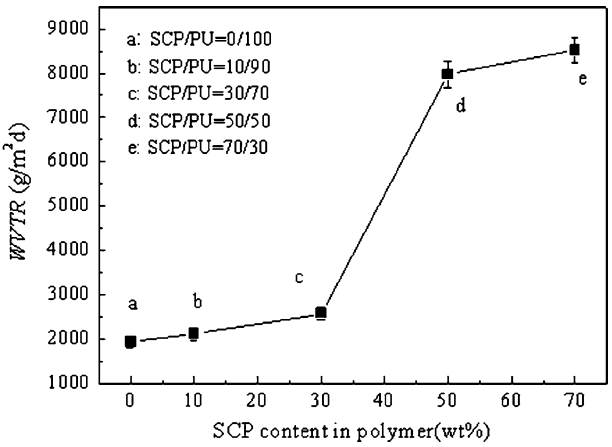

Fig. 7 WVTR of different SCP/PU blend membranes

vapor adsorption and diffusion in blend membranes. When SCP content increasing to 50 and 70 wt%, the porosities of blend membrane started to reduce, this depressed the diffusion rate of water vapor. But, a further increment of SCP content improved the hydrophilicity of blend membrane, which could accelerate the adsorption rate of water vapor in the blend membranes. Consequently, WVTR of blend membranes still increased further with SCP content in polymer reaching 50 and 70 wt%. In addition, when SCP content was very high, the –OH and $–NH_2$ groups of chitosan chains can interaction with –C=O and –NH– groups in PU chains by hydrogen bonds. Then the interaction of PU chains was weakened and amorphous region increased, which contributed to the permeation of water vapor.

Mechanical properties

The mechanical testing results are shown in Table 3. The result indicated that there was an obvious decrease in elongation at break, tensile strength at break and elastic modulus of the blend membranes with the ratio of SCP increasing. Especially, stress declined violently when the ratio of SCP reached 50 wt% in the membranes. Here, stress at break of blend membrane was only 20% of that of pure PU films, and there was more loss when ratio of powder was 70 wt%. The decrease in tensile property of blend membrane was due to the addition of SCP, which had destroyed the regular and uniform internal structure of PU. Firstly, compared with the PU soft continuous phase in the blend membranes, SCP as the dispersal phases were considered as the rigid particles that could result in stress-convergence. When the blend membranes were stretched, the points of the stress-convergence were damaged preferentially. Hence, the mechanical properties of SCP/PU blend membranes felled down with the SCP ration increasing. Secondly, from the appearances and the hand feeling of these blend membranes, it was easy to find that the membranes became more and more brittle as the more amount of the rigid SCP were added into the membranes, leading to the elongation, the intensity and modulus of the blend membrane reducing.

Table 3 Mechanical properties of blend membranes with different SCP contents

Membrane sample	SCP/PU (wt/wt)	Tensile strength at break (MPa)	Elongation at break (%)	Elastic modulus (MPa)
a	0/100	8.19 ± 0.76	385 ± 5	0.186 ± 0.003
b	10/90	7.71 ± 0.35	340 ± 3	0.250 ± 0.006
c	30/70	2.55 ± 0.35	300 ± 5	0.070 ± 0.005
d	50/50	1.66 ± 0.14	262 ± 8	0.059 ± 0.002
e	70/30	0.71 ± 0.09	220 ± 6	0.036 ± 0.004

Lastly, and the particle size of SCP kept in a micron level, consequently, some gaps as the interface pores could be observed at the interface between the powder and PU in the blend membranes. These gaps could be another reason for the loss in tensile properties of blend membrane. With 10% SCP, most powder was enwrapped by PU in the membrane, so the destruction effect was small. But, when the ratio of powder was above 30%, this destruction effect became more obvious. Whereas, even the ratio of powder reached 70%, the blend membrane also had good elasticity, i.e., 200% of elongation percentage.

Conclusion

In this study, a new type of composite materials was prepared by immersing the blend solutions of SCP and medical PU into the coagulation. SCP addition can alter the structure and performance of PU membrane. With an increment of SCP content, the pore diameter and porosities of blend membranes increased firstly, and decreased subsequently. However, the water absorption rate and WVTR were enhanced remarkably with SCP content increasing, which resulted from SCP strong hydrophilicity. WAXD results revealed that the aggregated structure of SCP was not destroyed and amorphous region of PU increased. The mechanical testing results indicated that with the increase in the ratio of SCP to PU, mechanical properties presented a downtrend for rigid chitosan powder created easily the stress-convergence points, whereas all blend membranes exhibited the good elasticity.

Acknowledgments The authors want to express their gratitude to the Major Grant of Hubei provincial department of education of China (No: Z200717001) for supporting this work.

References

1. Muzzarelli RAA (1993) Carbohydr Polym 20:7–16
2. Di Martino A, Sittinger M, Risbud MV (2005) Biomaterials 26:5983–5990
3. Singh DK, Ray AR (2000) J Macromol Sci C 40:69–83
4. Cheng M, Deng J, Yang F, Gong Y, Zhao N, Zhang X (2003) Biomaterials 24:2871–2880
5. Zhang H, Neau SH (2001) Biomaterials 22:1653–1658
6. Koyano T, Minoura N, Nagura M, Kobayashi K (1998) J Biomed Mater Res 39:486–490
7. Chuang WY, Young TH, Yao CH, Chiu WY (1999) Biomaterials 20:1479–1487

8. Khoo CGL, Frantzich S, Rosinski A, Sjöströmb M, Hoogstraate J (2003) Eur J Pharm Biopharm 55:47–56
9. Mucha M, Pawlak A (2005) Thermochim Acta 427:69–76
10. Zhai ML, Zhao L, Yoshii F, Kume T (2004) Carbohydr Polym 57:83–88
11. Sionkowska A, Wisniewski M, Skopinska J, Kennedy CJ, Wess TJ (2004) Biomaterials 25:795–801
12. Lin DT, Young TH, Fang Y (2001) Biomaterials 22:1521–1529
13. Pulat M, Senvar C (1995) Polymer Test 14:115–120
14. Shen Y, Shen X (2001) Fiber Ind Text 19:1–7
15. Novak S, Kobe S, McGuiness P (2004) Powder Tech 139:140–147
16. Pattanayak A, Sadham C (2005) Polymer 46:3275–3288
17. Li X, Lee J, Widya T (2005) Polymer 46:775–783
18. Freddi G, Tsukada M, Beretta S (1999) J Appl Polym Sci 71:1563–1571
19. Xu WL, Cui WG, Li WB, Guo WQ (2004) Powder Technol 140:136–140
20. Ma WZ, Zhang J, Wang XL, Wang SM (2007) Applied Surface Science 253:8377–8388
21. Kim JH, Min BR, Park HC, Won J, Kang YS (2001) J Appl Polym Sci 81:3481–3488
22. Huang JH (2007) Polymer Testing 26:685–691
23. Reuvers AJ, Smolders CA (1987) J Membr Sci 34(1):67–86
24. Mi FL, Shyu SS, Wu YB, Lee ST, Shyong JY, Huang RN (2001) Biomaterials 22:165–173